American Mineralogist, Volume 95, pages 126–134, 2010

Semi-ordered crystalline structure of the Santa Olalla vermiculite inferred from X-ray powder diffraction

Arancha Argüelles,[1,*] Matteo Leoni,[2] Jesús A. Blanco,[1] and Celia Marcos[3]

[1]Departamento de Física, Universidad de Oviedo, C/ Calvo Sotelo, s/n, 33007, Oviedo, Spain
[2]Department of Materials Engineering and Industrial Technologies, University of Trento, via Mesiano, 77, 38100 Trento, Italy
[3]Departamento de Geología e Instituto de Organometálica Enrique Moles, Universidad de Oviedo, C/ Jesús Arias de Velasco, s/n, 33005, Oviedo, Spain

Abstract

A sample of Mg-vermiculite from Santa Olalla (Spain) was studied by X-ray powder diffraction, electron microprobe, and thermo-gravimetry. The 3D structure is described as a disordered stack of two types of 2D building blocks, which are made up of one talc-type layer and one interlayer space containing hydrated Mg^{2+} cations. We have succeeded in the refinement of both the atomic positions and occupancies of exchangeable cations and water molecules in the interlayer space of this vermiculite using the program package DIFFaX+. The position of the Mg^{2+} cations is the only difference between the two layers. Besides the water molecules associated to the octahedrally coordinated Mg^{2+}, we also located water molecules in the interlayer space. The structural analysis confirms that vermiculite is a semi-ordered crystalline material characterized by the existence of a large density of defects due to random ~±*b*/3 translations along the crystalline [010] direction. In this way, this structure can no longer be described by means of a unit cell repeated in 3D space. Instead, long-range order is only recognized in the *a*-*b* plane. The 3D structure is described by means of a recursive method.

Keywords: Mg-vermiculite, stacking faults, X-ray diffraction, DIFFaX+

Introduction

Vermiculite is an interesting mineral both from the basic and applied point of view (Strand and Stewart 1983; Hindman 1992; Bergaya et al. 2006). The possibility of atomic intercalation makes it suitable for the sorption of heavy metals (Lee et al. 2002) and organic contaminants (Redding et al. 2002; Huang et al. 2005), whereas the low gas permeability (Takahashi et al. 2006) and the interesting mechanical properties (Tjong et al. 2002) renders vermiculite useful for the production of clay-based nanocomposites (Matějka et al. 2006).

Vermiculite is a 2:1 phyllosilicate, similar in appearance to mica. The thickness of the structural unit (assemblage of 2:1 layer and interlayer space) is about 14 Å, depending on the water interlamellar layers and the interlayer cations. Isomorphic substitutions in tetrahedral and/or octahedral positions are common.

The structure of natural vermiculite was first studied via X-ray powder diffraction (XRD) by Gruner (1934) who proposed a monoclinic *Cc* or *C*2/*c* cell. Hendricks and Jefferson (1938) confirmed Gruner's conclusions from single-crystal diffraction, but also suggested the presence of a partial random displacement of layers parallel to the *y*-axis. Subsequently, other authors (Mathieson and Walker 1954; Mathieson 1958) demonstrated that in Kenyan vermiculite water molecules and exchangeable cations occupy well-defined sites within the interlayer space. Shirozu and Bailey (1966) were able to add more details to the picture by working on a specimen from Llano as ordered structure (2-layer ordered structure, $c = 28.89$ Å): the shift between successive 2:1 layers is always of $-a/3$ along the **x**-axis and alternates between $+b/3$ and $-b/3$ along the **y**-axis. De la Calle et al. (1975a) concluded that the observed intensities and diffuseness of $k \neq 3n$ reflections in the Llano vermiculite indicate that many stacking faults are present, disrupting the regular alternation of $+b/3$ and $-b/3$ interlayer shifts. Thus de la Calle et al. (1988) proposed a random model alternating $\pm b/3$ shifts for a sample from Santa Olalla (Spain).

It is now well known that vermiculites have various possible layer-stacking sequences (de la Calle et al. 1975a, 1975b, 1978, 1985) depending on the nature of the interlayer cation and of relative humidity. Some systematization of the disorder sequences in vermiculites was presented by Weiss and Durovic (1980) using the order-disorder (OD) theory developed by Dornberger-Schiff (1956), based on the algebra of groupoids.

The reference state of Mg-vermiculites under natural conditions in the soil shows an average $d_{001} \sim 14.3$ Å (see e.g., Walker 1956; Zhou et al. 1993) and has both Mg^{2+} and two layers of water in the interlayer (2-water layer hydration state or 2-WLHS, notation after Suzuki et al. 1987).

By ordered phase, we mean one in which the position of any atom in the crystal follows both point group and space group symmetry. In layered materials (e.g., clays), disorder can however be present. This disorder can range from faulting in the sequence of one type of layer (random rotations and/or translations from one layer to the next, e.g., turbostratic disorder) to the presence of different kinds of layers randomly alternating in the stack (interstratified phases, see e.g., Marcos et al. 2003).

* E-mail: aranchajorge@telefonica.net

An ordered stack has hardly ever been found in vermiculites. Various studies (de la Calle et al. 1977; de la Calle and Suquet 1988) report on the key role of the interlayer species in determining the layer arrangement to preserve bonding and charge distribution in the interlayer. As in phlogopites, ordering in vermiculite occurs when the pseudohexagonal cavities (made of six-membered tetrahedra rings) are facing each other in adjacent tetrahedral layers. In this case, the 3D structure can be described using classical crystallographic methods, as all reflections are of the Bragg type (diffuse scattering is absent).

The structure of vermiculite is called semi-ordered when the transition from a layer to the next one can be obtained in two or more different ways (different translations along the **y**-axis). The translations along **x** and **z** are always –1/3 and 1, respectively, using the conventional cell. A schematic representation of a semi-ordered stacking mode with ±*b*/3 translation faults along the **y** direction is shown in Figure 1a. For semi-ordered stacks, the reciprocal space cannot be described by a set of *hkl* reciprocal points (with *h*, *k*, *l* integer), but rather by modulated reciprocal rods *hk* with continuous variation in the intensity along them that depends on the nature of the layers and the way they are stacked (de la Calle et al. 1988; Guinier 1964) (Fig. 1b). Note the presence of modulated reciprocal rods *hk* with $k \neq 3n$.

Faulted materials present unusual XRD patterns (Méring 1949; Hendricks and Teller 1942; Drits and Tchoubar 1990). Traditional analysis methods fail in describing the observed patterns owing to the extra features present in positions forbidden by the crystallography of a 3D regular lattice. Since the middle of the last century, several methods have been proposed to deal with the problem of random faulting (see e.g., Warren 1941; Brindley and Méring 1951; Warren and Bodenstein 1965), some of them leading to a successful simulation of the

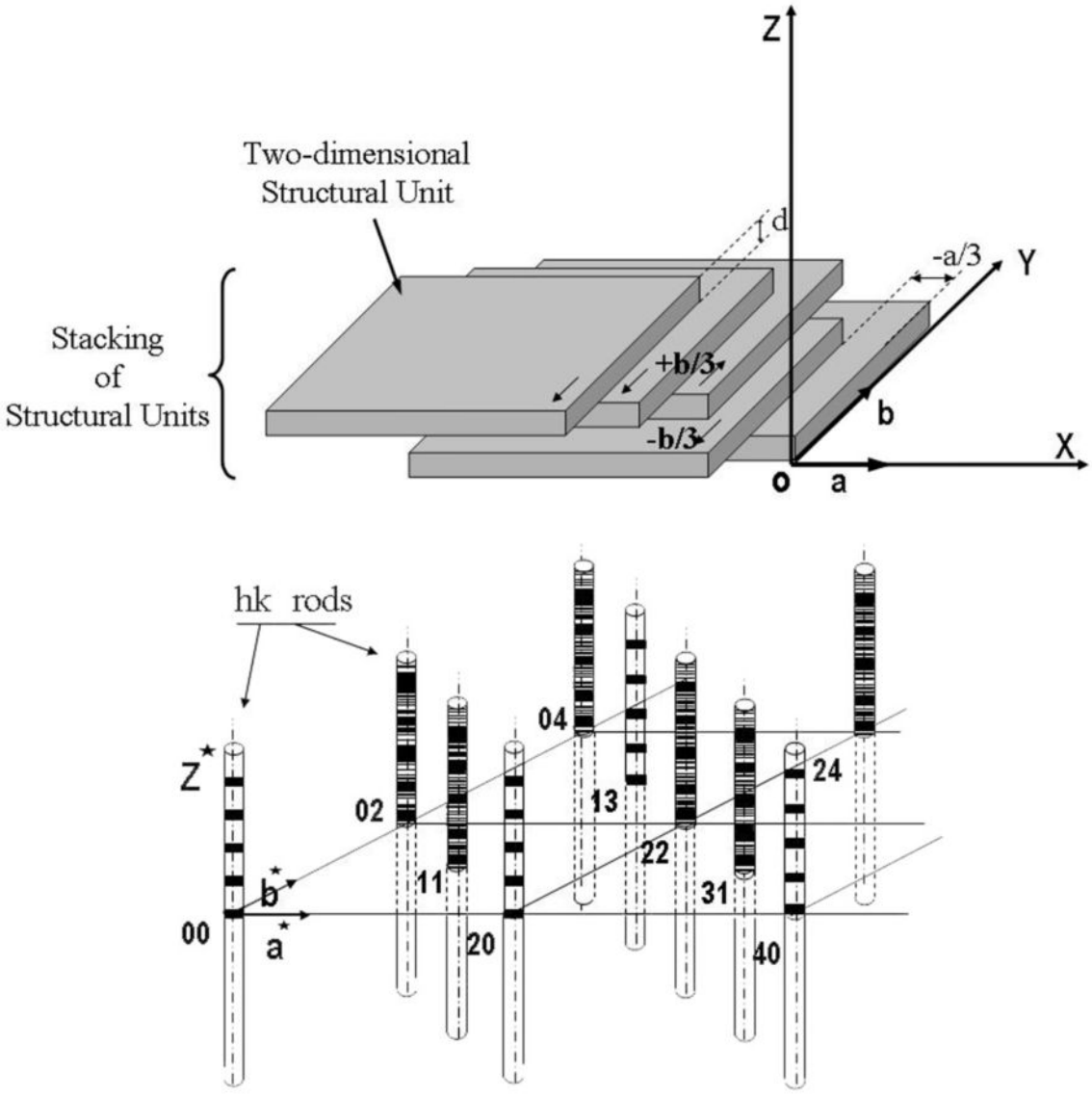

FIGURE 1. Schematic representation of a semi-ordered stacking mode with (±*b*/3) translation faults along the **y**-axis (**a**); rods in the reciprocal space for a semi-ordered structure (de la Calle et al. 1993; reproduced with permission) (**b**).

powder pattern of disordered layer structures (Hendricks and Teller 1942; Plançon and Tchoubar 1977; Pons et al. 1980; de Courville-Brenasin et al. 1981; Andreev and Lundström 1995; Plançon 2002). These approaches are, however, highly demanding from the computational point of view. Uffer et al. (2004) have proposed the possibility of simulating such patterns via fast aperiodic Fourier transform (Press et al. 1988), describing the structure of the faulted material through a supercell elongated on the stacking direction and containing several layers randomly translated one from each other.

A possible alternative is the formalism of Treacy et al. (1991), widely employed for simulating the powder patterns of faulted crystals as it is relatively fast and the software implementing it (DIFFaX) is readily available. The core of DIFFaX is a recursive description of the stacking, generalizing the works on Markov chains initiated by Hendricks and Teller (1942), Cowley (1976), Michalski (1988), and Michalski et al. (1988). DIFFaX has been successfully applied to analyze clay silicates (see, e.g., Artioli et al. 1995; Viani et al. 2002; Gualtieri 1999), although other software, such as WILDFIRE (Reynolds 1994) or NEWMOD (Reynolds 1985), are more widely accepted in the clay community.

Simulation and visual comparison between data and model is the common analysis method adopted in all studies mentioned so far. The refinement of faulted structures is, however, a more complex task and the relevant literature to date is scarce (de Courville-Brenasin et al. 1981). Recently, Leoni et al. (2004) added instrumental features and a nonlinear least squares refinement engine to DIFFaX, creating the DIFFaX+ code. Similar software was later independently proposed by Casas-Cabanas et al. (2006). In its latest revision (M. Leoni, personal communication), DIFFaX+ allows simulation and refinement of structural and microstructural features of any ≤3D periodic and modular structure. In this version, it has been already used for the refinement of the structure of another clay mineral, namely illite (Gualtieri et al. 2008). In the present study, DIFFaX+ has been used to confirm the stacking model of the Mg-vermiculite structure of Santa Olalla (Spain) from a powdered sample.

Experimental sample and methods

The sample analyzed in the present study is a natural Mg-vermiculite from Santa Olalla (Huelva, Spain). The origin and mineralogy of Santa Olalla vermiculite have been extensively investigated in the literature (González García and García Ramos 1960; Velasco et al. 1981; Justo et al. 1986; Luque et al. 1985), and it is widely accepted that this mineral is formed by transformation of phlogopite, the latter resulting from an alteration of pyroxenites. Also, it is accepted that Santa Olalla vermiculite is pure (without impurities due to others phyllosilicates), on the basis of their chemical composition and of the information obtained from the experimental X-ray powder pattern diffraction data (Justo et al. 1986, 1989; Marcos et al. 2003, 2004a, 2004b, 2009). The average composition of the sample is known from previous studies (Marcos et al. 2003, 2004b).

Thermogravimetric analysis (TGA) was employed to assess the actual water content. A Mettler-Toledo TGA/SDTA851 instrument was used to perform the analyses under dynamic nitrogen atmosphere (50 mL/min) at a heating rate of 10 °C/min, using an alumina crucible filled with 17.39 mg of vermiculite. Sample powder, with particle size < 80 μm, was obtained by 2-step rotor/screen system using a Retsch Ultra-Centrifugal Mill, ZM-1 model.

XRD patterns were collected both in reflection and in transmission geometry. A vertical Seifert XRD 3000 Bragg-Brentano diffractometer working with a copper tube (λ = 1.5418 Å) (40 kV, 30 mA) was employed for the measurement in reflection geometry, needed for 1D Fourier study. The diffractometer operates with a large radius (280 mm), secondary curved graphite monochromator, 2 mm divergence slit, 1 mm antiscatter slit, and 0.1 mm receiving slit. The illuminated area is ca. 20 mm × 20 mm on the specimen. The pattern was collected in the 4–105 °2θ range, with a step of 0.02° and a fixed counting time of 20 s per step. Due to the platelet-like shape of vermiculite grains, typical of most clays , a [00*l*] fiber texture is expected, with an enhancement of the signal from the basal planes.

A vertical INEL XRD RG3000 Debye-Scherrer goniometer operating a cobalt tube (λ = 1.7890 Å) (40 kV, 35 mA) and equipped with a curved position sensitive detector (INEL CPS 120) allowed the measurement of a transmission pattern in the 4–70 °2θ range (step 0.03°, 5400 s total acquisition time). The primary X-ray beam was focused on a 0.01 mm thick and 0.3 mm diameter glass capillary by a Johannson quartz monochromator (101 reflection, radius of curvature = 1400 mm, mis-cut = 8°). The nonlinearity of the INEL detector was corrected via software using the algorithm proposed by Roux and Volfinger (1996).

One-dimensional Fourier analysis was performed to determine the electron density profile ρ(*z*) along the **c** axis of the crystallographic unit cell. The reflection pattern (showing the basal Bragg-type reflections) was corrected for absorption, Lorentz and polarization factors (Brindley and Gillery 1956), to obtain the 00*l* Bragg intensities, I_{00l}, related to ρ(*z*) via the structure factor (*F*) (cf. Guinier 1964; Pons et al. 1989). Also and due to the size of sample a correction convert constant surface to constant energy has been done to avoid the overflow. The most reliable ρ(*z*), and thus the atomic distribution along the **z**-axis, was obtained by comparing the electronic density profile obtained from the observed structure factors, F_{obs}, with that obtained from the calculated structure factors, F_{calc}.

The DIFFaX+ software (Leoni et al. 2004) and the last version (M. Leoni, personal communication) were employed to refine the structure/microstructure. The material was described as a random sequence of two possible types of 2D layers (1 unit-cell thick) stacked along [001]. The starting *b* cell parameter was obtained from the isolated 060 reflection, whereas *a* was deduced by the $b/\sqrt{3}$ hexagonal relation. The 1D Fourier analysis finally provided the distance d_{001} between two unit blocks. Starting atomic positions, occupancy, and isotropic temperature factors were taken from the structural model published by de la Calle et al. (1988) with some minor corrections. Initial positions for the interstitial water molecules were proposed taking in mind the results reported by de la Calle et al. (1993) and Beyer and Reichenbach (1998). Structural parameters were then refined together with microstructural ones such as layer transition probabilities, translation vectors, and average domain size.

Results and discussion

The structural formula for a half unit cell of vermiculite from Santa Olalla has been previously reported by de la Calle (1977):

$$(Si_{2.718}Al_{1.282})(Mg_{2.593}Al_{0.059}Fe^{3+}_{0.236}Fe^{2+}_{0.029}Ti_{0.083})O_{10}(OH)_2(Mg_{0.388}Ca_{0.024})\cdot nH_2O$$

To account for chemical heterogeneity in the mineral deposit, the specimen studied in the present paper was re-analyzed by electron microprobe (Marcos et al. 2003) providing an average structural formula (again referred to a half unit cell and calculated on the basis of 10 structural O atoms):

$$(Si_{2.83}Al_{1.17})(Mg_{2.46}Al_{0.3}Fe_{0.22}Ti_{0.02})O_{10}(OH)_2(Mg_{0.38}Ca_{0.03}Na_{0.02})\cdot 3.815H_2O$$

The total water content was determined by TGA. The derivative of the mass loss curve (DTG curve in Fig. 2) shows two peaks at ca. 120 and 240 °C, respectively, corresponding to the various stages of dehydration of the interlayer. In particular, the first peak can be associated with the transformation from the 2-water to 1-water layer hydration state (2-WLHS to 1-WLHS), whereas the second corresponds to the transition from the 1-water to 0-water layer hydration state (1-WLHS to 0-WLHS), as already shown, e.g., by de la Calle and Suquet (1988). A detailed description of the arrangement of water molecules in the interlayer space for

the various hydration states can be found in the literature (see e.g., Mathieson and Walker 1954; Shirozu and Bailey 1966). A value of 5.87 water molecules per formula unit is found from the mass loss at ca. 120 °C, while a value of 1.76 water molecules is found from the step at ca. 240 °C.

The ratio between the number of H_2O molecules and the Mg^{2+} interlayer cations is 7.74 for the first transformation and 2.32 for the second. As it is assumed that the interlayer Mg-cations are octahedrally coordinated by the structural water (Mathieson and Walker 1954; Beyer and Reichenbach 1998; de la Calle et al. 1988), the expected ratio is 6 for 2-WLHS. An excess of 4.04 water molecules is therefore evidenced. This excess can be explained either by the presence of water molecules adsorbed on the surface and edges of the grains and/or by the presence of interstitial water molecules (see e.g., Skipper et al. 1991; Slade et al. 1998; Beyer and Graf von Reichenbach 1998). These authors propose several models to place these molecules into interlayer space. The mentioned models have been considered in this work, as it will be discussed later on, to interpret the results obtained with several techniques of X-ray diffraction and giving a satisfactory structural model for the analyzed sample.

Starting from the detected loss of mass to 120 °C a value of 2.94 H_2O molecules has been obtained by formula unit (f.u.), while 0.88 is the value deduced from the registered loss of H_2O molecules by f.u. for 240 °C. In total, the number of H_2O molecules/f.u. is equal to 3.82.

The X-ray powder diffraction patterns of the Santa Olalla vermiculite confirm the high purity of the sample because any signal from minerals usually associated with vermiculite (phlogopite or biotite) is absent, as also stated by Marcos et al. (2009). On the other hand, fitting of the basal reflections provides d_{001} = 14.36(2) Å, similar to that found in other Mg-vermiculites (see e.g., Walker 1956; Zhou et al. 1993).

Experimental values of structure factors F_{00l} were obtained from the intensities of the first 14 basal reflections by means of 1D Fourier analysis. The reliability factor R considered for the basal reflection was:

$$R = \frac{\sum_l \left| |F_{00l\,\mathrm{exp}}| - |F_{00l\,\mathrm{calc}}| \right|}{\sum_l |F_{00l\,\mathrm{exp}}|} 100\% \quad (1)$$

Atomic positions and occupancies derived from the structural model of de la Calle et al. (1988) were used in the study. To account for the TGA results, extra water molecules were positioned in the interlayer space, close to those coordinated to the Mg^{2+} cations. An initial guess of their z-coordinate was provided by the works of Beyer and Reichenbach (1998) and de la Calle et al. (1993). Figure 3 shows the corresponding theoretical and experimental electronic density profiles, ρ(z): an R factor of 7.5% was obtained, with a clear improvement in the fitting of the electron density ρ in the region around Mg^{2+} in the interlayer. Best-fit values of the z-coordinates (along the direction perpendicular to the basal a-b plane) of the extra water molecules are listed in Table 1. Since the occupancies of positions for the interstitial water molecules obtained from 1D Fourier analysis (3.78) are consistent with those obtained by TGA analyses (3.82) these parameters were also used with DIFFaX+.

The X-ray powder diffraction pattern collected in transmission geometry (see Fig. 4) does not show the strong orientation effects present in the corresponding pattern collected in reflection mode. The indexing of the diffractogram reveals the presence of some extremely asymmetric broadened peaks corresponding to 0k and 1k rods with $k \neq 3n$ (see Fig. 2b). The intensity distribution along hk reciprocal rods falls into two groups: (1) those h0

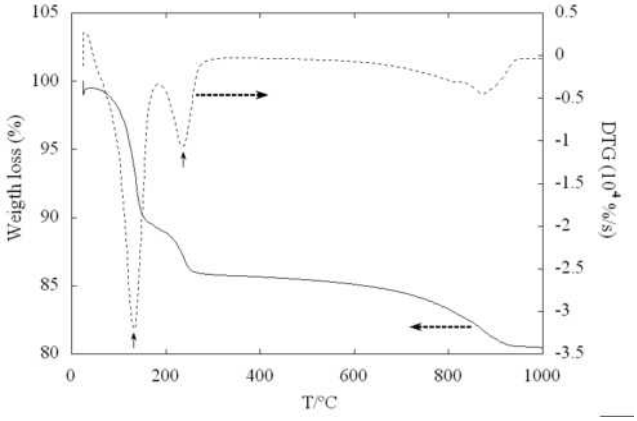

FIGURE 2. DTA/TG curves for powdered Mg-vermiculite from Santa Olalla. Temperature dependence of the weight loss (solid line) and the curve from differential thermal analysis (dashed line) showing two endothermic peaks at 120 and 240 °C, indicated by arrows.

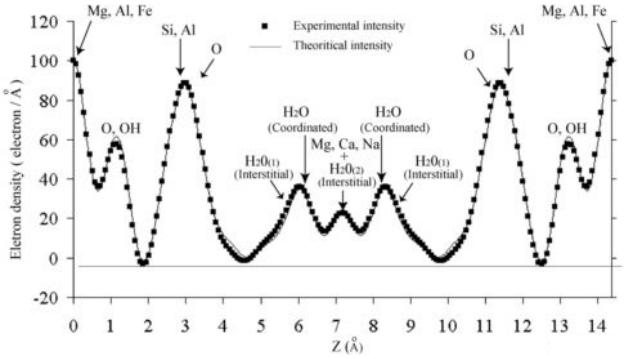

FIGURE 3. One-dimensional electron density distribution along the **z**-axis obtained by Fourier calculations. $H_2O_{(1)}$: water molecules of the coordination polyhedra of Mg^{2+}; $H_2O_{(2)}$: interstitial water molecules; Mg, O, OH, and Si atoms positions are also shown.

TABLE 1. The z-coordinate (along the direction perpendicular to the a-b plane) and occupancy values for the atoms of Mg-vermiculite from Santa Olalla, in a half layer, from the best fit obtained by Fourier analysis

	z (Å)	Site occupancy
T-O-T layer		
Mg, Fe, Al, Ti	0	3
Si, Al	2.72	4
O1	1.10	4
O2	3.30	4
O3	3.20	2
OH	0.90	2
Interlayer space		
Mg^{2+}, Ca^{2+}, Na^{+}	7.18	0.43
H_2O (coordinated)	6.07	2.58
H_2O1 (interstitial)	5.85	1.00
H_2O2 (interstitial)	7.18	0.20

Note: Zero at the Mg-octahedral site.

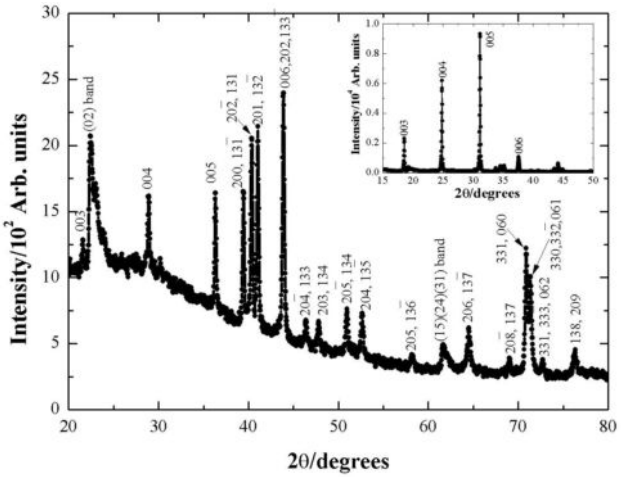

FIGURE 4. Co$K\alpha$ (λ = 1.7890 Å) X-ray powder diffraction pattern obtained in transmission geometry for an Mg-vermiculite from Santa Olalla at RT. These *hkl* indexes are assigned to the reflections. The inset shows an XRD pattern in reflection geometry (Cu$K\alpha$, λ = 1.5418 Å). Note that in transmission geometry all the allowed reflections are observed, whereas in reflection geometry only the basal 00*l* are clearly visible. Line is a guide for the eyes.

and 13 rods containing sharp (*h*0*l*, 13*l*) diffraction spots (Bragg-type reflections in Fig. 4), and (2) those with $k \neq 3n$ containing diffuse bands (asymmetric broadened peaks in Fig. 4). From these results, the *x*0*z* projection appears to be ordered, although the layers might be randomly displaced by ±*b*/3 parallel to the **y**-axis; as it was described by de la Calle et al. (1988) for the Santa Olalla vermiculite.

The impossibility of analyzing such data with a method based on the assumption that the lattice has 3D periodicity, is clear. This limitation is not present in the DIFFaX+ code, developed for the modeling of faulted structures. The starting model to be refined was built on the results of de la Calle et al. (1988) (relevant data listed in Table 2, CIF on deposit[1]). Atoms were mapped into an orthogonal cell perpendicular to the stacking direction as the most simple option with DIFFaX+. In this way, the building block for the stacked structure is a 2:1 (T-O-T) silicate layer whose interlayer space is filled with water molecules and exchangeable cations (Fig. 5).

Two types of layers (understanding by "layer" a structural unit consisting of a silicate layer and its interlayer space), A and B (de la Calle et al. 1988), are considered in the stack, differing in the position of the hydrated Mg-cations within the interlayer space. Four probabilities (defined in de la Calle et al. 1988) allow statistical characterization of the stacking model of A- and B-layers in a layer sequence. As can be seen in Figure 6, the exchangeable cations occupy the *m*1 position in the A-layer and the *m*2 position in the B-layer, respectively (cf. Mathieson and Walker 1954). For both positions, the water coordination polyhedron is located above the base of the SiO_4 tetrahedron. A third position proposed by Mathieson and Walker is *m*3, located above a ditrigonal cavity (cf. Figs. 6a and 6b).

Faulting in the studied Mg-vermiculite is assumed to occur by random translation of ±*b*/3 along the cell **y**-axis. Specifically, the A- and B-layers require a shift of +*b*/3 and –*b*/3, respectively, to allow for the hydrogen bonding of the water-coordination polyhedra with framework O atoms (cf. Figs. 7a and 7b). In both cases, the hydrated interlayer cation settles in between the bases of two tetrahedra.

In this work, we have also attempted to position water molecules in the interlayer space. Keeping in mind the *z*-coordinates deduced from the 1D Fourier analysis, and *x*- and *y*-coordinates given by Beyer and Reichenbach (1998) and de la Calle et al. (1993) for similar samples, we have proposed a starting model (see Fig. 8 and Table 2). According to TGA results two types of positions for this extra water content have been considered at first: (1) H_2O close to coordinated water molecules and therefore hydrogen bonding to them, and (2) H_2O close to several of the O atoms of the silicate tetrahedra, hydrogen bonding to them. The occupancies used were the ones deduced from the TGA and the 1D Fourier analysis, as it was previously mentioned. All of these parameters have been refined sequentially. The rest of the atomic positions were kept fixed as it is considered that the structure of the T-O-T layer is well established. Some of the coordinates have to be fixed as the quality of the X-ray data does not allow a convergent refinement. Refined parameters are those with uncertainties in parentheses in Tables 2 and 3.

With respect to the stacking parameters and to test the relative quality of the ordered and semi-ordered models to describe the structure of vermiculite against each other, different models in terms of transition probabilities between both type of layers, A and B, and the relative displacements between them, along the **y**-axis have been taken into account. One modeling attempt has been made supposing a translation of ±1/2 along the **y**-axis. The other models consider a translation of ±1/3, as usually observed in vermiculites (Argüelles et al. 2009). Different sequences of the stacking have been considered by changing the probabilities of layer to layer transition. In particular and according to the stacking model used in de la Calle et al. (1988), we define random mode as a random alternation of A and B type layers, and a segregated one as a sequence favoring one type of layer being followed by a layer of the same type, e.g., A-A or B-B. In all cases, a refinement was tried. The best fitting was obtained for a model in which the probability of a layer being followed by one of the same type is 0.42, a bit lower than in a totally random model, as previously proposed by de la Calle et al. (1988) (see Table 3). This seems to suggest that the energetic difference between the two layer-stacking sequences {A-A, B-B} and {A-B, B-A} is very small, slightly favoring the former, thus leading to a different environment for hydrogen bonding and the extra water molecules. Refined values for the translation vector in the **y**- direction are also listed in Table 3, showing no major departure from the starting ±*b*/3 values.

Besides disorder effects, the broadening of the diffraction peaks in the experimental pattern are mainly related to the finite size of the coherently diffracting domains, without microdis-

[1] Deposit item AM-10-004, CIF. Deposit items are available two ways: For a paper copy contact the Business Office of the Mineralogical Society of America (see inside front cover of recent issue) for price information. For an electronic copy visit the MSA web site at http://www.minsocam.org, go to the *American Mineralogist* Contents, find the table of contents for the specific volume/issue wanted, and then click on the deposit link there.

TABLE 2. Atomic parameters of the idealized orthogonal cell refined in DIFFaX+ for the A- and B-layers of Mg-vermiculite from Santa Olalla

	Atom	x/*a*	y/*b*	z/*c*	B (Å^2)	Site occupancy
			Silicate layer			
Octahedral cations	Mg	0	1/3	0.230[1)]	1	0.820
	Mg	0	2/3	0.230	1	0.820
	Mg	0	0	0.230	1	0.820
	Fe	0	1/3	0.230	1	0.073
	Fe	0	2/3	0.230	1	0.073
	Fe	0	0	0.230	1	0.073
	Al	0	1/3	0.230	1	0.100
	Al	0	2/3	0.230	1	0.100
	Al	0	0	0.230	1	0.100
	Ti	0	1/3	0.230	1	0.007
	Ti	0	2/3	0.230	1	0.007
	Ti	0	0	0.230	1	0.007
Tetrahedral cations	Si	0.331	1/3	0.419	1.5	0.708
	Si	0.331	2/3	0.419	1.5	0.708
	Si	0.669	1/3	0.04	1.5	0.708
	Si	0.669	2/3	0.04	1.5	0.708
	Al	0.331	1/3	0.419	1.5	0.292
	Al	0.331	2/3	0.419	1.5	0.292
	Al	0.669	1/3	0.04	1.5	0.292
	Al	0.669	2/3	0.04	1.5	0.292
Oxygen	O	0.326	1/3	0.309	1	1
	O	0.326	2/3	0.309	1	1
	O	0.674	1/3	0.15	1	1
	O	0.674	2/3	0.15	1	1
	O	0.062	0.269	0.460	2	1
	O	0.062	0.731	0.460	2	1
	O	0.938	0.269	0	2	1
	O	0.938	0.731	0	2	1
	O	0.37	1/2	0.453	2	1
	O	0.63	1/2	0.007	2	1
Hydroxyl group	OH	1/3	0	0.295	1	1
	OH	2/3	0	0.164	1	1
			Interlayer space			
A-layer *m*1	Mg	0.336	2/3	0.730	2.5	0.38(6)
	Mg	0.836	1/6	0.730	2.5	0.38(6)
	Ca	0.336	2/3	0.730	2.5	0.03
	Ca	0.836	1/6	0.730	2.5	0.03
	Na	0.336	2/3	0.730	2.5	0.02
	Na	0.336	2/3	0.730	2.5	0.02
	H_2O	0.004	2/3	0.652(2)	3	0.20(2)
	H_2O	0.004	0	0.652(2)	3	0.20(2)
	H_2O	0.004	1/3	0.652(2)	3	0.20(2)
	H_2O	0.540(8)	1/6	0.652(2)	3	0.20(2)
	H_2O	0.540(8)	1/2	0.652(2)	3	0.20(2)
	H_2O	0.540(8)	5/6	0.652(2)	3	0.20(2)
	H_2O	0.154	1/6	0.816(2)	3	0.20(2)
	H_2O	0.154	1/2	0.816(2)	3	0.20(2)
	H_2O	0.154	5/6	0.816(2)	3	0.20(2)
	H_2O	0.630(7)	2/3	0.816(2)	3	0.20(2)
	H_2O	0.630(7)	0	0.816(2)	3	0.20(2)
	H_2O	0.630(7)	1/3	0.816(2)	3	0.20(2)
			Interlayer space			
Interstitial water	H_2O1	0.062	0.269	0.59(2)	4.0	1/6
	H_2O1	0.062	0.731	0.59(2)	4.0	1/6
	H_2O1	0.370	1/2	0.59(2)	4.0	1/6
	H_2O1	0.605	0.064	0.85(2)	4.0	1/6
	H_2O1	0.605	0.602	0.85(2)	4.0	1/6
	H_2O1	0.297	0.833	0.85(2)	4.0	1/6
B-layer *m*2	Mg	0.336	1/3	0.730	2.5	0.38(6)
	Mg	0.836	5/6	0.730	2.5	0.38(6)
	Ca	0.336	1/3	0.730	2.5	0.03
	Ca	0.836	5/6	0.730	2.5	0.03
	Na	0.336	1/3	0.730	2.5	0.02
	Na	0.336	1/3	0.730	2.5	0.02
	H_2O	0.004	1/3	0.652(2)	3	0.20(2)
	H_2O	0.004	0	0.652(2)	3	0.20(2)
	H_2O	0.004	2/3	0.652(2)	3	0.20(2)
	H_2O	0.540(8)	5/6	0.652(2)	3	0.20(2)
	H_2O	0.540(8)	1/2	0.652(2)	3	0.20(2)
	H_2O	0.540(8)	1/6	0.652(2)	3	0.20(2)
	H_2O	0.154	5/6	0.801(2)	3	0.20(2)
	H_2O	0.154	1/6	0.801(2)	3	0.20(2)
	H_2O	0.154	1/2	0.801(2)	3	0.20(2)
	H_2O	0.630(7)	1/3	0.801(2)	3	0.20(2)
	H_2O	0.630(7)	2/3	0.801(2)	3	0.20(2)
	H_2O	0.630(7)	0	0.801(2)	3	0.20(2)
Interstitial water	H_2O1	0.062	0.269	0.59(2)	4.0	1/6
	H_2O1	0.062	0.731	0.59(2)	4.0	1/6
	H_2O1	0.370	1/2	0.59(2)	4.0	1/6
	H_2O1	0.605	0.398	0.85(2)	4.0	1/6
	H_2O1	0.605	0.936	0.85(2)	4.0	1/6
	H_2O1	0.297	1/6	0.85(2)	4.0	1/6

Notes: Cell parameter values are: a = 5.343(2) Å (in-plane), b = 9.254(2) Å (in-plane), and c = 14.34(3) Å (along stacking direction). All the atomic positions in the interlayer space are given in the table. Only half of the atoms in the T-O-T sandwich are listed. The complete cell is obtained by adding a second set of atoms with translation of [+1/2,+1/2,0] to those given in the table. These positions were not refined.

tortions. A different shape between basal reflection (narrower and with different symmetry) and the remaining peaks may be observed. This is an indication of a platelet-like (coin) domain shape. The best fit is obtained when assuming an infinite size (from the XRD point of view, i.e., larger than a few hundred nanometers) along the **a** and **b** crystallographic directions and an average platelet thickness of 40 layers (i.e., around 57 nm) (see Table 3). This lamellar domain shape is a typical feature of phyllosilicates, and it is consistent with the morphology of the crystallites.

Diffraction intensities were calculated for a statistical ensemble of crystallites, each with a distinct stacking sequence, though weighted by the probability that such a sequence will occur. The results of DIFFaX+ refinement are shown in Figure 9 (continuous line) and in Table 2. Polyhedra formed by the water-coordinated Mg^{2+} cations hardly differ from the starting model. The interstitial water molecules are placed near these polyhedra and the O atoms of the silicate tetrahedra to enable hydrogen bonds. Bond distances obtained within the interlayer between the interstitial molecule and the framework O atoms are consistent with the distances expected. The refined model matches the experimental data with a reliability factor R_{wp} = 6.46% (McCusker et al. 1999): the major features (both Bragg and diffuse) in the pattern are reproduced by the semi-ordered model. The shape of the lowest-2θ Bragg diffraction peak (7.2°) (see the inset of Fig. 9) exhibits a clear asymmetry caused probably by specimen transparency and flat surface. These effects may provoke large errors in line-broadening analysis and then this 2θ range has been omitted. As pointed out by Gualtieri et al. (2008) an improvement and optimization of the existing algorithms and programs are needed in order to establish a full picture of the structural and microstructural models.

The structure of Mg-vermiculite from Santa Olalla modeled by means of the DIFFaX+ software show extensive faulting due to nearly random ±*b*/3 translations along the [010] direction.

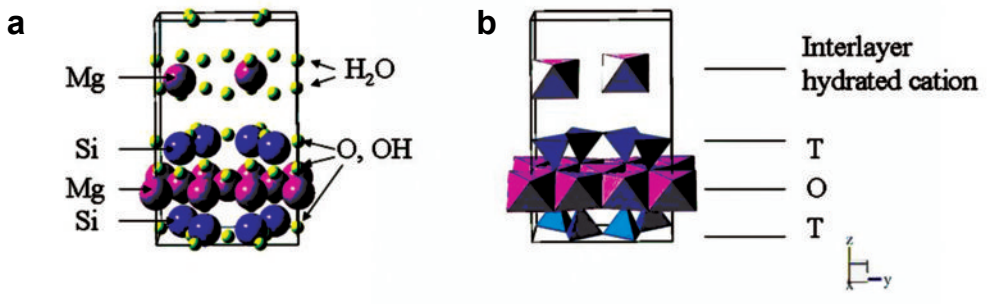

FIGURE 5. Schematic representation of the unit cell of Mg-vermiculite. (**a**) Detail of atoms in the T-O-T layer and the hydrated cations in the interlayer (Si = blue; Mg = pink; O, OH = yellow). (**b**) Coordinated tetrahedral and octahedral polyhedra and interlayer space. (Color online.)

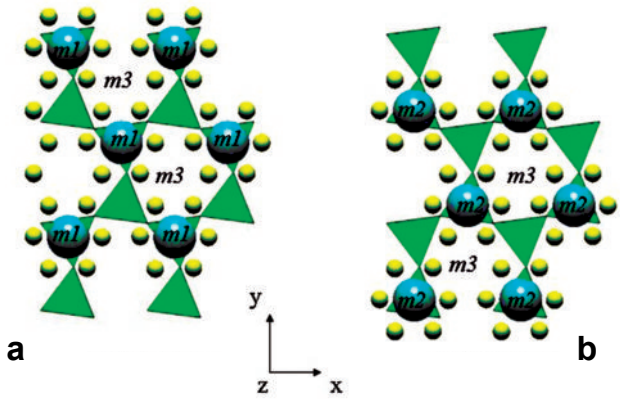

FIGURE 6. Section of the crystal structure of Santa Olalla Mg-vermiculite from $z = 0.310$ to $z = 0.806$ projected on the x-y plane of the crystallographic structure. Sites of Mg-exchangeable cations in the interlayer space indicating $m1$ and $m2$ sites in (**a**) the A-layer and (**b**) the B-layer, respectively (nomenclature of Mathieson and Walker 1954). These $m3$ sites are also shown in both figures.

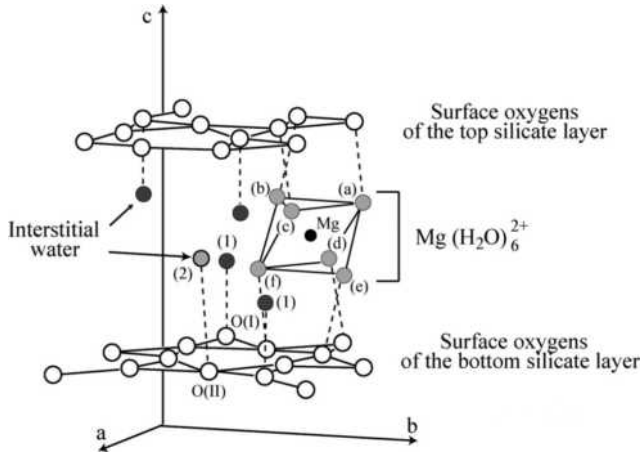

FIGURE 8. Schematic view of the interlayer space in Mg-vermiculite from Santa Olalla. As the occupancies of the suitable positions are less than unity, only one Mg-cation is considered in this picture. This view shows the space available to host interstitial water molecules of types 1 and 2 (see text).

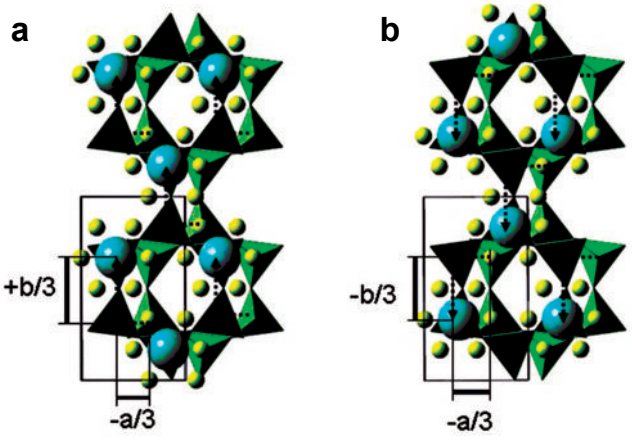

FIGURE 7. Relative positions of Mg-interlayer cations between two layers for the translations ($-a/3, \pm b/3, 1$). Section of the crystal structure from $z = 0$ to $z = 0.806$, projected onto the x-y plane of the crystallographic structure. For the sake of simplicity, only tetrahedra of T-O-T bonds and interlayer hydrated cations are drawn. Translations ($-a/3, +b/3, 1$) and ($-a/3, -b/3, 1$) forced, respectively, by the A- and B-layers (Mg-cations in the $m1$ and $m2$ positions, respectively) are indicated in **a** and **b**, respectively, by dashed arrows. Light green tetrahedra for the next layer (not drawn in the figure) must be translated along the dashed arrows. (Color online.)

TABLE 3. Parameters used in the DIFFaX+ software calculations

Parameter	Description	Refined values
a (Å)	Cell parameter, in-plane	5.343(2)
b (Å)	Cell parameter, in-plane	9.254(2)
d_{001} (Å)	Cell parameter, along stacking direction	14.34(3)
Number of layers (**c** direction)	Number of layers (**c** direction)	40(3)
$t_{yA\rightarrow A}$ (Å)	Translation from one layer to the next (y-axis)	0.339(1)
$t_{yA\rightarrow B}$		0.336(2)
$t_{yB\rightarrow A}$		–0.323(2)
$t_{yB\rightarrow B}$		–0.332(2)
α_{AA}	Transition probability from layer-A to layer-A	0.42(1)
α_{AB}	Transition probability from layer-A to layer-B	0.58(1)
α_{BA}	Transition probability from layer-B to layer-A	0.58(1)
α_{BB}	Transition probability from layer-B to layer-B	0.42(1)

Notes: Starting structural values from de la Calle et al. (1988), instrumental settings and refined structural parameters for the best model (see text). Angles as well as translation along **x**-direction were kept fixed. Peak widths were refined using the angle dependent relation FWHM = $U\tan 2\theta + V\tan\theta + W$ yielding U = 0.777(7), V = –0.725(4), and W = 0.212(2).

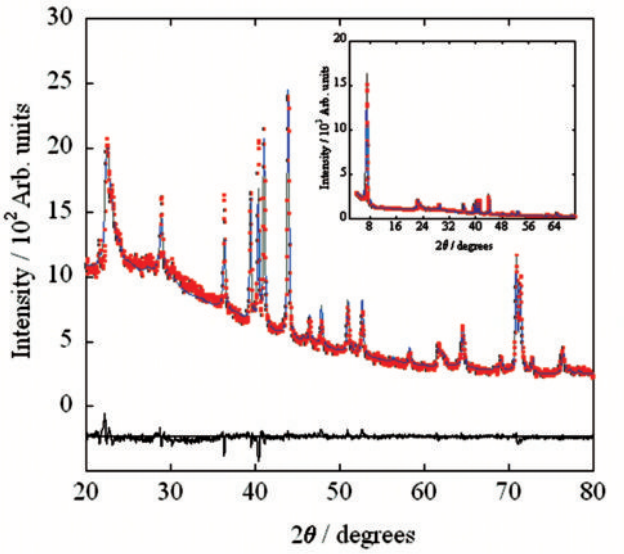

FIGURE 9. Experimental (red points) and calculated diffraction (blue line) pattern obtained by the DIFFaX+ software with a 3D-structure model for vermiculite including interstitial water molecules in the interlayer space. Experimental pattern collected in transmission geometry at RT (see text). Wider 2θ-range (4–70°) of the diffraction pattern is shown in the inset (see text), in which the reflections only correspond to the crystalline structure of vermiculite (JCPDS card 16-613), with the most characteristic reflection observed at 6.2 °2θ. (Color online.)

Thus the semi-ordered model obtained in this work by X-ray powder diffraction confirms the previously model obtained by de la Calle et al. (1988).

ACKNOWLEDGMENTS

The authors acknowledge the Servicios Científico-Técnicos de la Universidad de Oviedo (Spain) for X-ray diffractometry, electron microprobe, and TGA analyses. The Institute des Sciences de la Terre d'Orléans (France) is also acknowledged for diffraction measurements in transmission geometry. The authors specially acknowledge Cristina de la Calle and Charles H. Pons and the reviewers for the critical reading of this paper and theirs comments. This work was supported from FEDER and the Spanish MICINN (former MEC) (Project no. MAT2008-06542-C04-03).

REFERENCES CITED

Andreev, Y.U. and Lundström, T. (1995) Simulation of powder diffraction diagrams from disordered and imperfect graphitic layers. Journal of Applied Crystallography, 28, 534–539.

Argüelles, A., Leoni, M., Pons, C.H., de la Calle, C., Blanco, J.A., and Marcos, C. (2009) Structure and microstructure of Mg-vermiculite. Zeitschrift für Kristallographie, Supplement 30, 429–434.

Artioli, G., Bellotto, M., Gualtieri, A.F., and Pavese, A. (1995) Nature of structural disorder in natural kaolinites: A new model based on computer simulation of powder diffraction data and electrostatic energy calculation. Clay and Clay Minerals, 43, 438–445.

Bergaya, F., Theng, B.K.G., and Lagaly, G. (2006) Handbook of Clay Science, p. 501–541. Elsevier, Amsterdam.

Beyer, J. and Graf von Reichenbach, H. (1998) Dehydration and rehydration of vermiculites: IV. Arrangements of interlayer components in the 1.43 nm and 1.38 nm hydrates of Mg-vermiculite. Zeitschrift für Physikalische Chemie, 207, 67–82.

Brindley, G.W. and Gillery, F.H. (1956) X-ray identification of chlorite species. American Mineralogist, 41, 169–181.

Brindley, G.W. and Méring, J. (1951) Diffractions des rayons X par les structures en couches de Desordonnees. I. Acta Crystallographica, 4, 441–447.

Casas-Cabanas, M., Rodríguez-Carvajal, J., and Palacín, M.R. (2006) FAULTS, a new program for refinement of powder diffraction patterns from layered structures. Zeitschrift für Kristallographie, Suppl. 23, 243–248.

Cowley, J.M. (1976) Diffraction by crystals with planar faults. I. General theory. Acta Crystallographica, A32, 83–87.

de Courville-Brenasin, J., Joyez, G., and Tchoubar, D. (1981) Méthode d'adjustement automatique entre courbes expérimentale et calculée dans les diagrammes de diffraction de poudre. Cas des solides à structure lamellaire. I. Développement de la méthode. Journal of Applied Crystallography, 14, 17–23.

de la Calle, C. (1977) Structure des Vermiculites. Facteurs conditionnant les mouvements des feuillets. Ph.D. thesis, Université Paris VI, France.

de la Calle, C. and Suquet, H. (1988) Vermiculite. In S.W. Bailey, Ed., Hydrous Phyllosilicates (Exclusive of Micas), 19, p. 455–496. Reviews in Mineralogy, Mineralogical Society of America, Chantilly, Virginia.

de la Calle, C., Dubernat, J., Suquet, H., Pezerat, H., Gaulthier, J., and Mamy, J. (1975a) Crystal structure of two-layer Mg-vermiculites and Na-, Ca-vermiculites. In S.W. Bailey, Ed., Proceedings of the International Clay Conference, Mexico City, p. 201–209. Applied Publishing, Wilmette, Illinois.

de la Calle, C., Suquet, H., and Pezerat, H. (1975b) Glissement de feuillets accompagnant certains echanges cationiques dans les vermiculites. Bulletin du Groupe Français des Argiles, 27, 31–49.

de la Calle, C., Pezerat, H., and Gasperin, M. (1977) Problèmes d'ordre désordre darts les vermiculites—Structure du minéral calcique hydratè à 2 couches. Journal de Physique, 38, 128–133.

de la Calle, C., Suquet, H., Dubernat, J., and Pezerat, H. (1978) Mode d'Empilement des feuillets dans les vermiculites hydratees a 'deux couches.' Clay Minerals, 13, 275–297.

de la Calle, C., Suquet, H., and Pezerat, H. (1985) Vermiculites hydratees a une couche. Clay Minerals, 20, 221–230.

de la Calle, C., Suquet, H., and Pons, C.H. (1988) Stacking order in a 14.30 Å Mg-vermiculite. Clays and Clay Minerals, 36, 481–490.

de la Calle, C., Martín de Vidales, J.L., and Pons, C.H. (1993) Stacking order in a K/Mg interstratified vermiculite from Malawi. Clays and Clay Minerals, 41, 580–589.

Dornberger-Schiff, K. (1956) On order-disorder structures (OD-structures). Acta Crystallographica, 9, 593–601.

Drits, V.A. and Tchoubar, C. (1990) X-ray Diffraction by Disordered Lamellar Structures, p. 233–303. Springer Verlag, New York.

González García, F. and García Ramos, G. (1960) On the genesis and transformations of vermiculite. Transactions 7th International Congress of Soil Science, Madison, Wisconsin. International Society of Soil Science, 4, 482–491.

Gruner, J.W. (1934) The structures of vermiculites and their collapse by dehydration. American Mineralogist, 19, 557–575.

Gualtieri, A.F. (1999) Modeling the nature of disorder in talc by simulation of X-ray powder patterns. European Journal of Mineralogy, 11, 521–532.

Gualtieri, A.F., Ferrari, S., Leoni, M., Grathoff, G., Hugo, R., Shatnawi, M., Paglia, G., and Billinge, S. (2008) Structural characterization of the clay mineral illite-1M. Journal of Applied Crystallography, 41, 402–415.

Guinier, A. (1964) Thèorie et Technique de la Radiocristallographie, p. 65. Dunod, Paris.

Hendricks, S.B. and Jefferson, M.E. (1938) Crystal structure of vermiculites and mixed vermiculite-chlorites. American Mineralogist, 23, 851–862.

Hendricks, S.B. and Teller, E. (1942) X-ray interference in partially ordered layer lattices. Journal of Chemical Physics, 10, 147–167.

Hindman, J.R. (1992) Vermiculite. Vermiculite Technology, Newsletter, 3A, 12 p.

Huang, H.C., Lee, J.F., Chao, H.P., Yeh, P.W., Yang, Y.F., and Liao, W.L. (2005) The influences of solid-phase organic constituents on the partition of aliphatic and aromatic organic contaminants. Journal of Colloid Interface Science, 286, 127–133.

Justo, A., Maqueda, C., and Pérez Rodriguez, J.L. (1986) Estudio químico de vermiculitas de Andalucía y Badajoz. Boletín Sociedad Española de Mineralogía, 9, 123–129.

Justo, A., Maqueda, C., Pérez Rodriguez, J.L., and Morillo, E. (1989) Expansibility of some vermiculites. Applied Clay Science, 4, 509–519.

Lee, J.J., Choi, J., and Park, J.W. (2002) Simultaneous sorption of lead and chlorobenzene by organobentonite. Chemosphere, 49, 1309–1315.

Leoni, M., Gualtieri, A.F., and Roveri, N. (2004) Simultaneous refinement of structure and microstructure of layered materials. Journal of Applied Crystallography, 37, 166–173.

Luque, F.J., Rodas, M., and Doval, M. (1985) Mineralogía y génesis de los yacimientos de vermiculita de Ojen. Boletín de la Sociedad Española de Mineralogía, 8, 229–238.

Marcos, C., Argüelles, A., Ruíz-Conde, A., Sánchez-Soto, P.J., and Blanco, J.A. (2003) Study of the dehydration process of vermiculites by applying a vacuum pressure: Formation of interstratified phases. Mineralogical Magazine, 67, 1253–1268.

Marcos, C., Rodríguez, I., Clauzio de Rennó, L., and Paredes, J.I. (2004a) Vermiculite surface structure as imaged by contact mode AFM. European Journal of Mineralgy, 16, 597–607.

Marcos, C., Ruíz-Conde, A., Argüelles, A., Sánchez-Soto, P.J., García, A., and Blanco, J.A. (2004b) Nuevos avances en la formación de fases interestratificadas durante el proceso de deshidratación-rehidratación de vermiculitas-Mg: Influencia de la presión de vacío, temperatura y composición. Boletín de la

Sociedad Española de Cerámica y Vidrio, 43, 138–140.
Marcos, C., Arango, Y.C., and Rodríguez, I. (2009) X-ray diffraction studies of the thermal behavior of commercial vermiculites. Applied Clay Science, 42, 368–378.
Matějka, V., Šupová-Křístková, M., Kratošová, G., and Valášková, M. (2006) Preparation of Mg-vermiculite nanoparticles using potassium persulfate treatment. Journal of Nanoscience and Nanotechnology, 6, 2482–2488.
Mathieson, A.M. (1958) Mg-vermiculite: A refinement of the crystal structure of the 14.36 Å phase. American Mineralogist, 43, 300–304.
Mathieson, A.M. and Walker, G.F. (1954) Crystal structure of magnesium-vermiculite. American Mineralogist, 39, 231–255.
McCusker, L.B., Von Dreele, R.B., Cox, D.E., Louër, D., and Scardi, P. (1999) Rietveld refinement guidelines. Journal of Applied Crystallography, 32, 36–50.
Méring, J. (1949) L'interfèrence des rayons X dans les systemes a stratification dèsordonnèe. Acta Crystallographica, 2, 371–377.
Michalski, E. (1988) The diffraction of X-rays by close-packed polytypic crystals containing single stacking faults. I. General theory. Acta Crystallographica, A44, 640–649.
Michalski, E., Kaczmarek, S., and Demianiuk, M. (1988) The diffraction of X-rays by close-packed polytypic crystals containing single stacking faults. II: Theory for hexagonal and rhombohedral structures. Acta Crystallographica, A44, 650–657.
Plançon, A. (2002) New modeling of X-ray diffraction by disordered lamellar structures, such as phyllosilicates. American Mineralogist, 87, 1672–1677.
Plançon, A. and Tchoubar, C. (1977) Determination of structural defects in phyllosilicates by X-ray diffraction. II: Nature and proportion of defects in natural kaolinites. Clays and Clay Minererals, 25, 4368.
Pons, C.H., Tchoubar, C., and Tchoubar, D. (1980) Organisation des molandules d'eau fi la surface des feuillets dans un gel de montmorillonites Na. Bulletin de la Societe Francaise de Mineralogie, 103, 452–456.
Pons, C.H., Pozzuoli, A., Rausell-Colom, J.A., and de la Calle, C. (1989) Mecanisme de passage de l'etat hydrate a une couche a l'etat "zero couche" d'une vermiculite-li de Santa-Olalla. Clay Minerals, 24, 479–493.
Press, W.H., Flannery, B.P., Teukolsky, S.A., and Vettering, W.T. (1988) Numerical Recipes in C. The Art of Scientific Computing, p. 427–428. Cambridge University Press, U.K.
Redding, A.Z., Burns, S.E., Upson, R.T., and Anderson, E.F. (2002) Organoclay sorption of benzene as a function of total organic carbon content. Journal of Colloid Interface Science, 250, 261–264.
Reynolds Jr., R.C. (1985) NEWMOD, A computer program for the calculation of one-dimensional diffraction patterns of mixed-layer clays. Hanover, New Hampshire.
——— (1994) WILDFIRE: A computer program for the calculation of three-dimensional X-ray diffraction patterns for mica polytypes and their disordered variations. Hanover, New Hampshire.
Roux, J. and Volfinger, M. (1996) Mesures precises a l'aide d'un detecteur courbe. Journal de Physique, VI C4, 6, 127–134.
Shirozu, H. and Bailey, S.W. (1966) Crystal structure of a two-layer Mg-vermiculite. American Mineralogist, 51, 1124–1143.
Skipper, N.T., Soper, A.K., and McConnell, J.D.C. (1991) The structure of interlayer water in vermiculite. Journal of Chemical Physics, 94, 5751–5760.
Slade, P.G., Self, P.G., and Quirk, J.P. (1998) The interlayer structure of La-vermiculite. Clays and Clay Minererals, 46, 629–635.
Strand, P.R. and Stewart, E. (1983) Vermiculites. In S.J. Lefond, Ed., Industrial Mineral and Rocks, p. 1375–1381. The Society of Mining Engineers of the American Institute of Mining, Metallurgical and Petroleum Engineers, New York.
Suzuki, M., Wada, N., Hines, D.R., and Whittingham, M.S. (1987) Hydration states and phase transitions in vermiculite intercalation compounds. Physical Review B, 36, 2844–2851.
Takahashi, S., Goldberg, H.A., Feeney, C.A., Karim, D.P., Farrell, M., O'Leary, K., and Paul, D.R. (2006) Gas barrier properties of butyl rubber/vermiculite nanocomposite coatings. Polymer, 47, 3083–3093.
Tjong, S.C., Meng, Y.Z., and Hay, A.S. (2002) Novel preparation and properties of PP-vermiculite nano composite. Chemistry of Materials, 14, 44–51.
Treacy, M.M.J., Newsam, J.M., and Deem, M.W. (1991) A general recursion method for calculating diffracted intensities from crystals containing planar faults. Proceedings of the Royal Society of London A, 433, 499–520.
Uffer, K., Roth, G., Kleeberg, R., Stanjek, H., Dohrmann, R., and Bergmann, J. (2004) Description of X-ray powder pattern of turbostratically disordered layer structures with a Rietveld compatible approach. Zeitschrift für Kristallographie, 219, 519–527.
Viani, A., Gualtieri, A.F., and Artioli, G. (2002) The nature of disorder in montmorillonite by simulation of X-ray powder patterns. American Mineralogist, 87, 966–975.
Velasco, F., Casquet, C., Ortega Huerta, M., and Rodríguez Gordillo, J. (1981) Indicio de vermiculita en el skarn magnético (aposkarn flogopítico) de La Garrenchosa (Sta. Olalla, Huelva). Sociedad Española de Mineralogía, 2, 135–149.
Walker, G.F. (1956) Mechanism of dehydration of Mg-vermiculite. Clays and Clay Minerals, 4, 101–115.
Warren, B.E. (1941) X-Ray diffraction in random layer lattices. Physical Review, 59, 693–698.
Warren, B.E. and Bodenstein, P. (1965) The diffraction pattern of fine particle carbon blacks. Acta Crystallographica, 18, 282–286.
Weiss, Z. and Durovic, S. (1980) OD interpretation of Mg-vermiculite. Symbolism and X-ray identification of its polytypes. Acta Crystallographica, A36, 633–640.
Zhou, P., Amarasekera, J., Solin, A., Mahanti, S.D., and Pinnavaia, T.J. (1993) Magnetic properties of vermiculite intercalation compounds. Physical Review, B, 47, 486–493.

MANUSCRIPT RECEIVED MARCH 20, 2009
MANUSCRIPT ACCEPTED SEPTEMBER 10, 2009
MANUSCRIPT HANDLED BY PAUL SCHROEDER